

Predicting soil properties in 3D: Should depth be a covariate?

Yuxin Ma ^{a,b,*}, Budiman Minasny ^a, Alex McBratney ^a, Laura Poggio ^c, Mario Fajardo ^a

^a Sydney Institute of Agriculture, School of Life and Environmental Sciences, The University of Sydney, 1 Central Avenue, 2015 Eveleigh, New South Wales, Australia

^b Landcare Research, Private Bag 11052, Manawatu Mail Centre, Palmerston North 4442, New Zealand

^c ISRIC - World Soil Information, Droevedaalsesteeg 3, 6708 PB Wageningen, The Netherlands

ARTICLE INFO

Handling Editor: Jan Willem Van Groenigen

Keywords:

Digital soil mapping

3D mapping

Average prediction interval

Tree-based model

ABSTRACT

Soil is a three-dimensional volume with property variability in all three dimensions. In Digital Soil Mapping (DSM), the variation of soil properties down a profile is usually harmonised by the use of the equal-area spline depth function approach. Soil observations at various depth intervals are harmonised to pre-determined depth intervals. To create maps of soil at the defined depth intervals, 2.5D model produces maps of individual depth intervals separately. Those maps can be reconstructed to produce a continuous depth function for each predicted location. More recently, several studies propose that soil property at any depth can be mapped using a model incorporating depth along with spatial covariates as predictor variables, creating a '3D' model. The aim of this study is to evaluate the proposition that soil properties can be predicted at any depth. This study compares the 2.5D model and 3D model in two areas. The first test is on a 1500 km² area in Edgeroi, New South Wales (NSW), Australia, mapping soil organic carbon (SOC, %), carbon storage (kg m⁻²), pH (H₂O), clay content (%), and cation exchange capacity (CEC, mg/kg) based on depth-interval observations. The second study area in the Lower Hunter Valley has SOC observations at every 2 cm increment from a 210 km² area. 2.5D and 3D models were tested in both study areas using four machine learning techniques: Cubist regression tree, Quantile Regression Forest (QRF), Artificial Neural Network (ANN), and 3D Generalised Additive Model (GAM). Results show that, in terms of R² and RMSE, 2.5D and 3D models using different machine learning models produce comparable results on the validation of depth interval observations. The 3D tree-based models produce "stepped" prediction of properties with depth. Results on the Hunter Valley area with point observations show that the 3D model cannot replicate field point observations. 3D soil mapping on point depth observation has lower accuracy and larger uncertainty compared to the 2.5D model. For future DSM studies, 3D soil mapping with depth as a covariate requires caution with respect to the prediction method and the requirements of the results.

1. Introduction

Soil is a dynamic, natural, three-dimensional (3D) body at the earth's surface with variability in property in all three dimensions (Hole, 1953; Poggio and Gimona, 2014). Soil is a key component of the ecosystems and is crucial for food, water and energy security, maintaining biodiversity, mitigating climate change, and influencing human health (McBratney et al., 2014). Soil function can be threatened by human activities, e.g. acceleration of soil erosion, soil contamination and soil salinisation. Consequently, it can result in environment detriment, economic and social damage. To assess and solve these problems, quantitative characterisation of key soil properties both in the vertical dimension through the soil profile and in the lateral dimension across landscapes is necessary (Ma et al., 2019a; Veronesi, 2012). This implies

the creation of detailed, high resolution, low uncertainties 3D digital soil maps for spatially modelling soil variation in all its spatial dimensions.

Digital soil mapping (DSM) (McBratney et al., 2003) approach has been applied to predict the spatial distribution of soil properties based on the relationships between soil properties and environmental factors with a variety of numerical approaches (Minasny and McBratney, 2016; Padarian et al., 2020). Techniques used varied from simple linear models to complex machine learning techniques, such as Cubist (Ma et al., 2019b), Random Forest (Breiman, 2001; Grimm et al., 2008), Artificial Neural Networks (Behrens et al., 2005), and deep learning (Padarian et al., 2019; Wadoux et al., 2019).

DSM models commonly produce two-dimensional (2D) maps of soil properties at single depth intervals or horizons (Malone et al., 2018). However, the depth interval of soil observations can vary between

* Corresponding author at: Landcare Research, Private Bag 11052, Manawatu Mail Centre, Palmerston North 4442, New Zealand.

E-mail addresses: yuxin.ma@sydney.edu.au, may@landcareresearch.co.nz (Y. Ma).

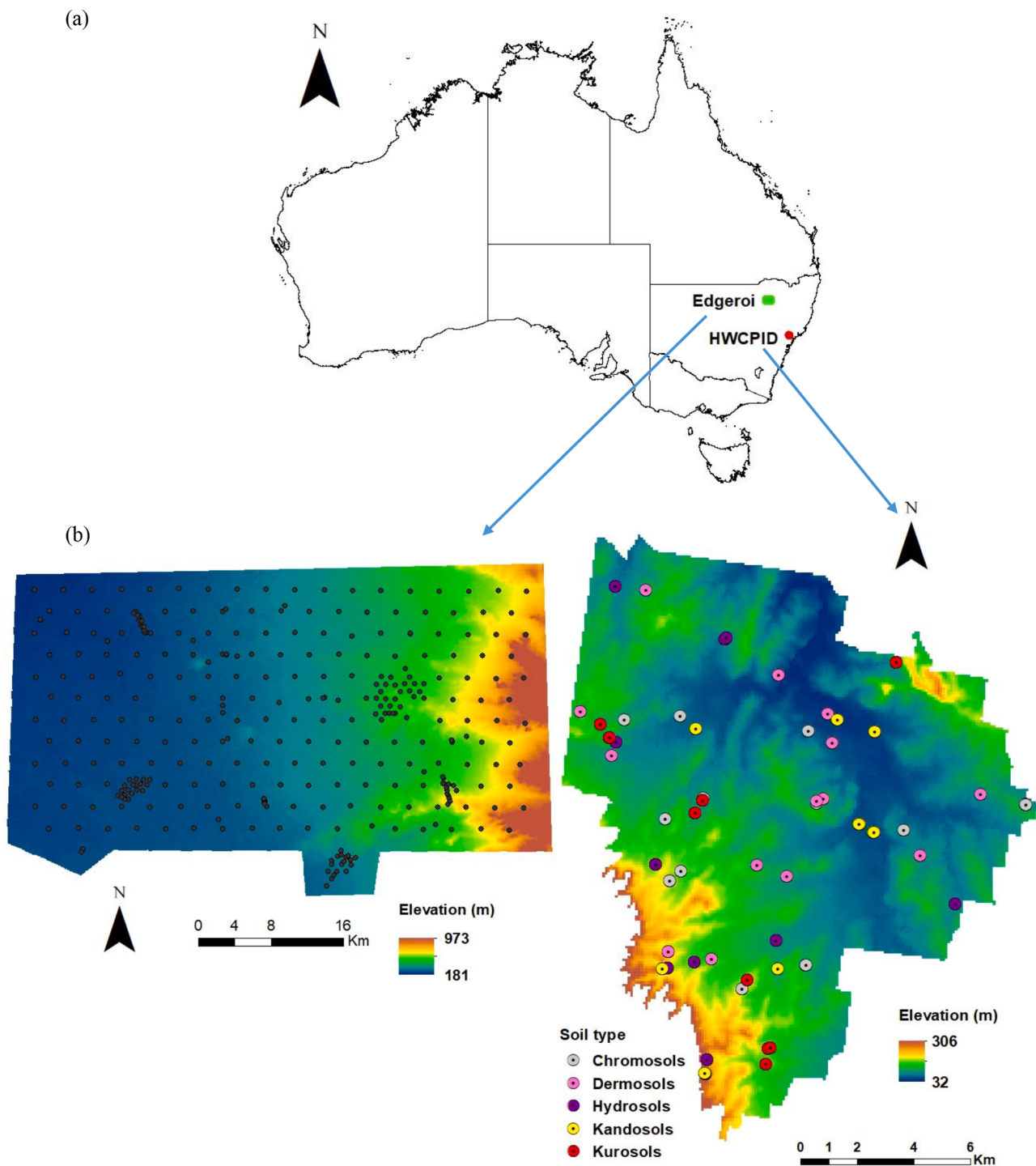


Fig. 1. Location of the two study sites (a) and the sampling points in each area (b).

locations or study area. The GlobalSoilMap project (Arrouays et al., 2014) defined six standard depth intervals of 0–5 cm, 5–15 cm, 15–30 cm, 30–60 cm, 60–100 cm and 100–200 cm as a way to standardise soil properties mapping.

A common way to facilitate mapping soil properties with depth intervals of the GlobalSoilMap specification has been depth harmonisation via the equal-area spline function (Malone et al., 2009). This equal-area spline model is based on the assumption that soil observations are taken from a depth interval, and a change of measurement support is required to harmonise soil observations (Bishop et al., 1999). Once the soil depth data have been harmonised, properties at each depth interval can be

mapped using the DSM approach. In addition, a continuous depth function can be recreated for each pixel based on the predicted depth interval values following the quadratic equal-area spline function (Lacoste et al., 2014).

Studies by Adhikari et al. (2014) and Kidd et al. (2015) are examples of the coupling of spline depth function with DSM to predict soil properties based on the GlobalSoilMap specification. These separate depth interval models commonly used different combinations of covariates. One of the limitations is that data from predictions at one depth do not influence predictions at another (Hengl et al., 2014). The approach by combining multiple 2D mapping is referred to as pseudo-3D mapping

(Liu et al., 2016) or 2.5D mapping.

The emerging 3D geostatistical modelling approach has been appealing for 3D mapping as it reduces the complexity of workflow (Malone et al., 2018). The one-step approach was able to refrain from resampling soil depths to specific depth intervals and integrate soil profile observations into one statistical analysis. For example, 3D GAM (Generalized Additive Model) coupled with 3D kriging (Poggio and Gimona, 2014), area-to-point kriging (Orton et al., 2016), and increment-averaged kriging (Orton et al., 2020).

Other studies modelled soil properties as parametric depth functions, for example, soil carbon is a negative exponential depth function (Minasny et al., 2006). The advantage of using depth function is that parameters of the function can be predicted by DSM techniques, such as modified neural network approach (Minasny et al., 2006), ordinary kriging (Mishra et al., 2009), or REML-EBLUP (residual maximum likelihood-empirical best linear unbiased predictor) geostatistical model (Veronesi, 2012). Once the parameters have been obtained, values at any depth can be calculated. However, these functions are only useful for certain soil properties that naturally follow certain functions down the soil profile, such as soil organic matter or carbon, total nitrogen and soil weathering rate, that show depth-exponential relationship. Clay content shows accumulation (maxima) with depth (Ma et al., 2019a; Malone et al., 2018). Pedologically, the most appealing approach, the horizon depth function method from Kempen et al. (2011) combined pedologically defined soil depth functions with geostatistical modelling. However, the aforementioned approach is limited to landscape contexts or soil types.

Recent studies proposed that a soil property at any depth can be mapped using a model incorporating depth along with spatial covariates as predictor variables (Akpa et al., 2014; Filippi et al., 2020, 2019; Hengl et al., 2017; Ramcharan et al., 2018; Zhang et al., 2020). The so-called 3D model has an assumption that observation from a depth interval is assumed to be equal as a point observation. This method changes the vertical support of the measurement from a depth interval to a single depth value. In comparison to the 2.5D approach, the full 3D approach modelling seems more efficient and flexible for producing spatial predictions at any location at any required depth. However, the accuracy and uncertainty in predictions by including depth as a covariate are still unclear. Nauman and Duniway (2019) compared the 2D and 3D approaches in terms of accuracy and uncertainty for mapping soil electrical conductivity (salinity), pH, the sum of fine and very fine sands, and organic carbon of soil pedogenic horizon depth using Random Forests based on the relative prediction interval (RPI) approach. Their results indicated that 3D mapping of soil properties with strong variation with depth could result in substantial areas predicted with much higher uncertainty than coincide with unrealistic predictions relative to the 2D model. However, they did not investigate the vertical distribution of soil property with depth and did not discuss the issue of the change of support.

This study aims to evaluate the proposition that soil properties can be evaluated at any depth by comparing the multi-layered 2.5D and 3D modelling. Three methods were compared to convert depth interval observations to point depths for the 3D approach. Four different machine learning models: Cubist regression tree, Quantile Regression Forest (QRF), Artificial Neural Network (ANN), and 3D Generalised Additive Model (GAM), were used to predict the distribution of five different key soil properties (soil organic carbon (SOC, %), carbon storage (kg m^{-2}), pH (H_2O), clay content (%), and cation exchange capacity (CEC, mg/kg)) with depth interval data from the Edgeroi area in eastern Australia. In addition, we also validate 2.5D and 3D models on an area in the Hunter Valley, Australia, where we have soil observations that were measured at every 2 cm.

2. Materials and methods

2.1. Study areas

This study used data from two sites in New South Wales (NSW), Australia (Fig. 1a). The first area is situated at Edgeroi area, in the lower valley of the Namoi River, near Narrabri, approximately 500 km northwest of Sydney. This area covers approximately 1500 km² and it is a typical part of the North-western Slopes and Plains of NSW (Minasny et al., 2006; Ward, 1999). Elevations within the study area range from 181 to 973 m (Fig. 1b, left). Predominant land use is agriculture, including irrigated cotton, wheat and pastoral farming. Native vegetation (partly forest and partly grassland) areas are mostly concentrated on the lower foothills of the Nandewar Range on the eastern flanks of the study site (Malone et al., 2009; Ward, 1999). The main basement rocks of the area are composed of Pilliga Sandstone, Nandewar and Garrawilla volcanics, and clayey sands of the Purlawaugh Formation, which are overlain by the calcareous Rolling Downs Group and a soft Tertiary sandstone (Ward, 1999). Further to the west, expansive alluvial plains dominate the area, by which more than 80% have slopes of less than 3° (Triantafilis and McBratney, 1993).

The second area is located at Pokolbin, in the Lower Hunter Valley, approximately 140 km north of Sydney with a total area of about 210 km². Geologically the area is situated in the Sydney basin, including predominantly Early Permian siltstones, marl, and some minor sandstone (Hawley et al., 1995) and Late Permian siltstones, Middle Permian conglomerates, sandstones and siltstones in small amounts. Topographically the majority of the study area consists of undulating hills and plains, which rises to low mountains on the southwest perimeter (Ma et al., 2019b). Elevation ranges from 32 to 306 m (Fig. 1b, right). The land use across the study area primarily dedicated to native pasture and irrigated viticulture, and native forest along the southern and western boundaries.

2.2. Soil data

The dataset from the Edgeroi consisted of 341 soil profiles, from which 210 were arranged in a systematic, equilateral triangular grid with approximately 2.8-km spacing between sites (McGarry et al., 1989), and an additional 131 were distributed more irregularly or on transects (Fig. 1b, left). The soil profiles were mainly Vertosols, followed by Dermosols, Sodosols, Calcarosols, Chromosols and Kandosols according to the Australian Soil Classification system (Isbell, 2002) or Vertisols, Luvisols/Acrisols, Solonetz, Calcisol, Lixisol/Luvisols, Ferralsols (IUSS Working Group WRB, 2014). The dataset included vegetation and landform information and soil attributes (morphological, physical and chemical data) at depths: 0–0.1, 0.1–0.2, 0.3–0.4, 0.7–0.8, 1.2–1.3 and 2.5–2.6 m. This study focuses on examining the vertical variabilities of soil organic carbon (SOC, %), total carbon storage (kg m^{-2}), pH (H_2O), clay content (%) and cation exchange capacity (CEC, mg/kg) with the depth of the soil profiles across Edgeroi at the time of observation (1985–1987). SOC was calculated as the difference between total carbon determined by combustion using a dry combustion method and carbonate carbon (Minasny et al., 2006). Total soil organic carbon storage was computed for the 0–30, 0–50 and 0–80 cm soil layers with the following equation (Poggio and Gimona, 2014):

$$\text{Total soil organic carbon storage} = \sum_{i=1}^n BD_i SOC_i (1 - VST_i) thick_i \quad (1)$$

where i is the i_{th} soil layer for a given depth (0–30, 0–50 and 0–80 cm layer), n is the number of soil layers, BD_i is soil bulk density (kg m^{-3}), SOC_i is the SOC concentration (%), VST_i is the volume percentage of rock fragments (%), and $thick_i$ is the thickness of i_{th} soil layer (m).

The dataset from the Hunter Valley consisted of 59 soil cores varying between 85 and 130 cm depth (Fajardo et al. (2016) (Fig. 1b, right). The

Table 1

List of the environmental covariates and their source for the two study sites.

Study area	Type of data	Environmental covariates	Source
Edgeroi	Digital elevation model	Elevation Slope Topographic wetness index (TWI) Multiresolution Ridge Top Flatness (MrRTF) Flow path length (FPL) Area above channel network (AOCN)	SRTM
	Remote sensing	Landsat 7 Normalized Difference Vegetation Index (NDVI) Soil enhancement ratios of b3/b2, b3/b7, b5/b7	Landsat
	Gamma-ray radiation	Abundance of potassium (⁴⁰ K) Abundance of thorium (²³² Th) Abundance of uranium (²³⁸ U)	Gamma-radiometric survey
	Digital elevation model	Elevation Slope Aspect TWI MrRTF Terrain ruggedness index (TRI) Terrain position index (TPI) Multiresolution Index of Valley Bottom Flatness (MrVBF) Stream power index (SPI) Melton ruggedness number (MRN) Slope Length and Steepness Factor (LS-factor) Relative Slope Position (RSP) Valley depth	SRTM
	Remote sensing	Landsat 7 NDVI	Landsat
	Soil	Soil type	Soil survey
	Gamma-ray radiation	Abundances of ⁴⁰ K Abundances of ²³² Th Abundances of ²³⁸ U	Gamma-radiometric survey

cores were taken based on a Latin hypercube sampling design (Minasny and McBratney, 2006) considering the compound topographic index, parent material and normalized difference vegetation index to maximize the variability of the samples. The soils are Chromosols, Dermosols, Hydrosols, Kandosols and Kurosols according to the Australian Soil Classification system (Isbell, 2002), which are equivalent to Lixisols/Luvisols, Acrisols, Gleysols, Ferralsols and Alisols according to WRB (IUSS Working Group WRB, 2014). The cores were air-dried and scanned at every 2 cm depth using a portable visible-near infrared (vis-NIR) spectrophotometer at wavelength 350 to 2500 nm with Agrispec instrument (Analytical Spectral Devices, Boulder Colorado) using a Spectralon® white tile as a reference reflectance. 100 samples from the soil cores at different depths were air-dried at room temperature (20–22 °C), removed stones/gravels and debris and then sieved to pass a 2 mm sieve. SOC concentration of the 100 samples was determined using the dry combustion method. The vis-NIR spectra were calibrated to predict SOC from the 100 samples. The validation for the prediction of SOC provided an R² value of 0.90 and a concordance correlation coefficient (pc) of 0.94. The calibration model was then applied to all samples with the vis-NIR spectra, resulting in a dataset of 2782 measurements of SOC every 2 cm until 1 m. The detail of this vis-NIR measurement and calibration can be found in Fajardo et al. (2016).

2.3. Environmental variables

The environmental covariates used to predict the selected soil

attributes for the Edgeroi site were resampled to a 90 m resolution (see Malone et al., 2009 for further details). The covariates used included (Table 1): 1) The digital elevation model (DEM) derived from the Shuttle Radar Topography Mission (SRTM) terrain data and terrain attributes, i.e. slope, topographic wetness index (TWI), Multiresolution Ridge Top Flatness (MrRTF), flow path length (FPL) and area above channel network (AOCN) derived from the DEM; 2) Landsat 7 with the Enhanced Thematic Mapper Plus (ETM+) from the year 2003 with bands 1, 2, 3, 4, 5 and 7 (b1, b2, b3, b4, b5 and b7). The Normalized Difference Vegetation Index (NDVI) was determined by the ratio between (b4 - b3) and (b4 + b3) as an indicator of the vegetation cover and type. Furthermore, the soil enhancement ratios of b3/b2, b3/b7, b5/b7 were derived which are able to accentuate carbonate radicals, ferrous iron, and hydroxyl radicals in exposed soil (Saunders and Boettiger, 2006); 3) The abundances of potassium (⁴⁰K), thorium (²³²Th) and uranium (²³⁸U) gamma-ray radiation of the earth surfaces from the gamma-radiometric survey (Geosciences Australia, 2008).

The environmental variables considered in Hunter Valley included (Table 1): Landsat 7 ETM+, DEM and terrain attributes derived from the DEM, i.e. slope, aspect, TWI, NDVI, MrRTF, terrain ruggedness index (TRI), terrain position index (TPI), Multiresolution Index of Valley Bottom Flatness (MrVBF), stream power index (SPI), Melton ruggedness number (MRN), Slope Length and Steepness Factor (LS-factor), Relative Slope Position (RSP), valley depth, soil type and the abundances of ⁴⁰K, ²³²Th and ²³⁸U. All covariates were used at a spatial resolution of 90 m.

2.4. Depth data processing

In the 2.5D approach, observed depth intervals were converted to GlobalSoilMap standard depth intervals using the equal-area spline. In the 3D approach, the observed depth intervals were converted to point depth observation based on three approaches described in the following subsections.

2.4.1. Depth intervals standardization – 2.5 D

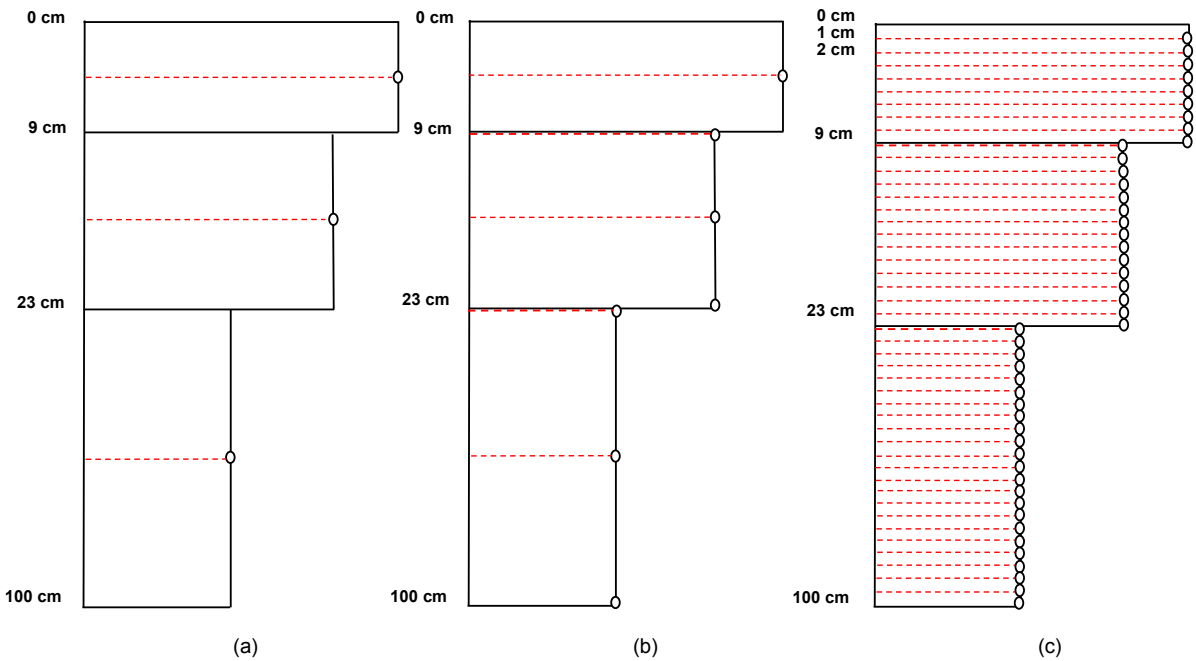
For the soil samples collected from different layers at Edgeroi, mass preserving spline functions (Bishop et al., 1999; Malone et al., 2009) were fitted individually to each profile for each property to resample the vertical profile data for the standardized depth increments of 0–5, 5–15, 15–30, 30–60, and 60–100 cm. This was implemented using the ‘ithir’ package (Malone, 2018) in the R statistical language (R Development Core Team, 2017). Separate DSM models were created for each spline fitted depth interval for the 2.5D approach.

The 2 cm measurements in Hunter Valley were aggregated into standardised depth interval measurements arithmetically (0–5, 5–15, 15–30, 30–60, and 60–100 cm). These values were used as observations to fit the 2.5D and 3D models.

2.4.2. Depth intervals converted to point depth – 3 D

For the 3D modelling, point values at certain depths were derived from depth interval soil observations. Depth was included in the model as a predictor variable. Three possible approaches were used so far to assign point-depth values and referred to 3D-A, 3D-B and 3D-F in this study.

- 1) Average: Depth values were assigned as the centre of the observed depth interval, (e.g., 4.5 cm for 0–9 cm depth interval) (Akpa et al., 2014) (Fig. 2a).
- 2) Average + Boundary: Depth values were assigned as the mid-point of the pedogenic horizons and the upper and lower boundaries of the horizon (Hengl and MacMillan, 2019). As some of the observations are 8 cm, if the first horizon is less than 9 cm, only the mid-depth was considered (Fig. 2b).
- 3) Fine discretization: Depth values were assigned at every centimetre of the depth intervals (Filippi et al., 2019) (Fig. 2c).



Possible approaches to assigning depth values.

Fig. 2. Possible approaches to assigning depth values.

2.5. Prediction models

Four machine learning techniques were evaluated and tested to model soil property observations from environmental variables: Cubist regression tree, Quantile Regression Forest (QRF), Artificial Neural Network (ANN) for 2.5D and 3D modelling approaches, and 3D Generalised Additive Model (GAM) for the 3D approach. Cubist, QRF and 3D GAM were implemented in R in the “Cubist” package (Kuhn et al., 2018), “quantregForest” package (Meinshausen, 2017) and “mgcv” package (Wood, 2019) respectively. These models were chosen because that Cubist and QRF models are popular tree-based model used within the DSM community. ANN, a parametric model, has been used to predict soil property at several soil depths simultaneously (Wadoux et al., 2019). The 3D GAM is a flexible smooth interpolator for 3D modelling examined by Poggio and Gimona (2014).

2.5.1. Cubist

Cubist is a rule-based model which allows one to explore nonlinear relationships in observed data. It is a tree model algorithm based on the M5 theory (Quinlan, 1992) and partitions the predictor variates into different subsets according to a series of “if-then” rules with each rule representing a multivariate linear model of the predictor (Kuhn et al., 2016). The Cubist algorithm has three parameters: rules, committees and extrapolations. The number of rules could potentially partition the data, and the extrapolation is a useful model constraint feature. In this study, we used 5 rules, 5% of data extrapolations and 10 committees, which suggested that 10 boosting iterations were used to obtain a prediction.

2.5.2. Quantile regression Forest (QRF)

Random Forest (Breiman, 2001) is a tree-based ensemble method, which operates by constructing a multitude of regression trees in predictor variables at each node by bootstrapping sampling and aggregating the individual trees to give one single prediction for each observation in a dataset. QRF (Meinshausen, 2006) is an extension of Random Forest which allows for nonparametric estimation of conditional quantiles of the prediction. In this study, we used 100 trees and

defaults of randomForest regression model package (Liaw and Wiener, 2018) for QRF.

2.5.3. Artificial neural networks (ANNs)

ANNs are parallel computing systems developed to simulate just the way the human brain processes information, based on the structure and functional aspects of biological neural networks, capable of fitting nonlinear relationships. A neural network consists of a system of many processing units, analogous to neurons, which have similar characteristics and arranged into layers and joined together by weights (Minasny and McBratney, 2002). In this study, multilayer perceptron (MLP) with multiple outputs was considered and trained in the software JMP®. It is a feedforward artificial neural network and consists of three layers: input, hidden and output layers, having 19 nodes for inputs (covariates), three hidden nodes and five outputs (0–5, 5–15, 15–30, 30–60, and 60–100 cm) for 2.5D model. For the 3D model, the 19 covariates plus depth were used as inputs (20 inputs), three hidden nodes, and a single output. The hyperbolic tangent sigmoid function was used as an activation function in the hidden nodes.

2.5.4. 3D Generalised Additive model (GAM)

GAM (Hastie and Tibshirani, 1986; 1990) is a generalisation of multiple regression by replacing the linear function of the explanatory variables with nonparametric smoothing techniques, such as splines to identify and represent possible nonlinear relationships between the soil properties and the considered covariates. Poggio and Gimona (2014) fitted a GAM to estimate the trend of SOC, using a 3D smoother with related covariates and kriging or Gaussian simulations of GAM residuals as a spatial component to account for local details to predict SOC at each cell for each of the considered depth layers. Here we only used 3D GAM fitting as follows:

$$S_p = f_1(N_p, E_p, D_p) + f_2(DEM_p) + f_3(TWI_p) + \dots + f_n(\dots) \quad (2)$$

where S_p is the values of soil properties at position p , f_1 is the multidimensional smooth function of the coordinates of the location (northing N and easting E) and depth D , f_2 to f_n are a one-dimensional smooth

Table 2

Accuracy statistics from true validation on the pedogenic horizons of the 103 profiles in Edgeroi.

Soil properties	Model	QRF		Cubist		ANN		3D GAM	
		R ²	RMSE						
SOC (%)	2.5D	0.44	0.51	0.45	0.51	0.46	0.50		
	3D-A	0.42	0.52	0.42	0.52	0.37	0.54	0.45	0.51
	3D-B	0.43	0.52	0.40	0.53	0.39	0.53	0.42	0.52
	3D-F	0.47	0.50	0.43	0.52	0.38	0.54	0.39	0.53
pH	2.5D	0.52	0.80	0.54	0.78	0.53	0.79		
	3D-A	0.53	0.79	0.49	0.82	0.53	0.79	0.51	0.80
	3D-B	0.53	0.79	0.45	0.85	0.51	0.81	0.45	0.85
	3D-F	0.53	0.79	0.45	0.85	0.46	0.84	0.48	0.83
Clay (%)	2.5D	0.37	12.91	0.38	12.79	0.41	12.54		
	3D-A	0.36	13.01	0.38	12.83	0.47	11.90	0.35	13.12
	3D-B	0.36	13.00	0.39	12.69	0.37	12.90	0.39	12.75
	3D-F	0.35	13.15	0.35	13.10	0.39	12.75	0.37	12.90
CEC (mg/kg)	2.5D	0.29	140.95	0.35	135.74	0.42	127.68		
	3D-A	0.31	139.58	0.32	138.40	0.35	135.27	0.30	140.25
	3D-B	0.29	141.63	0.34	136.17	0.39	130.64	0.28	142.44
	3D-F	0.30	140.61	0.30	140.47	0.39	130.53	0.29	141.38

function of the values of the covariate at the considered location. By using the “bam” function in R, the number of basis dimension, k which determines the maximum complexity of each smoother (covariates), sets a maximum for the estimated Effective Degrees of Freedom (EDF) for the smoothers. This function also requires a smoothing parameter λ estimated via fast REML. In this study, k was determined using cross-validation.

2.6. Validation

The 341 soil profiles in Edgeroi were partitioned into a training set and a validation set to assess the quality of the prediction model. 70% (238 profiles) were selected randomly as a training set and the remaining (103 profiles) as a validation set. Due to the limited profile data in Hunter Valley, we conducted a profile-based 10-fold cross-validation by dividing randomly the 59 soil cores into 10 groups and then training a model using 90% of profiles and the remaining profiles were left out during each fold model fitting. As described by Nauman and Duniway (2019) and Ramcharan et al. (2018), this cross-validation

makes the training and validation sets independent by leaving out all horizons in a profile in fold test sets, as opposed to horizon-based cross-validation (Hengl et al., 2017) where the accuracy of unsampled locations could be overly optimistic.

Each soil property, values at every 1 cm were reconstructed from the 2.5D modelling predictions using the equal-area spline model. For the 3D model, prediction at every 1 cm was calculated directly. For the Edgeroi dataset, the predictions were calculated to the depth interval of observations and compared. For the Hunter Valley site, the comparisons were made on the 2 cm point observations. Coefficient of determination (R^2) and root mean square error (RMSE) were used to evaluate the performance of the approaches.

2.7. Uncertainty analysis

Uncertainty was calculated for SOC prediction models in the Hunter Valley by predicting the 5th and 95th percentiles using the QRF approach. QRF gives a nonparametric estimate of conditional quantiles prediction based on the bootstrapped trees. The difference between 95th

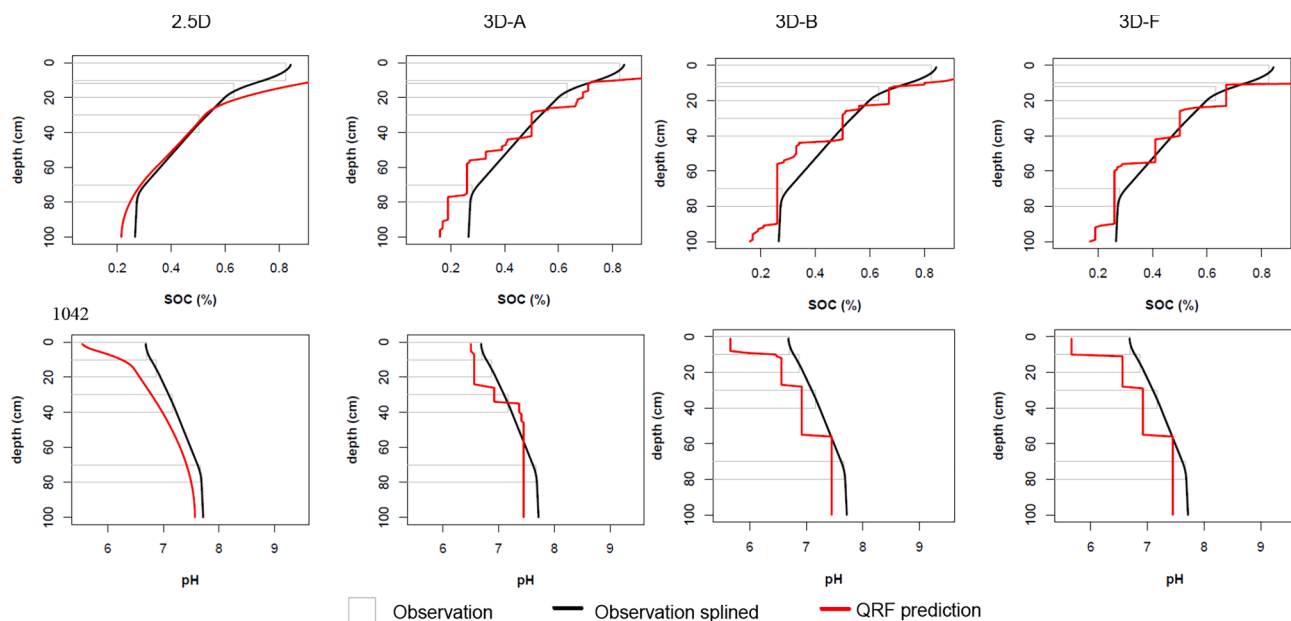


Fig. 3. Plots of 2.5D and 3D predictions versus observed values of SOC (profile: ed343) and pH (profile: na036). Grey box is observation, the black line is observation splined using mass preserving spline functions, and the red line is QRF prediction. (For interpretation of the references to colour in this figure legend, the reader is referred to the web version of this article.)

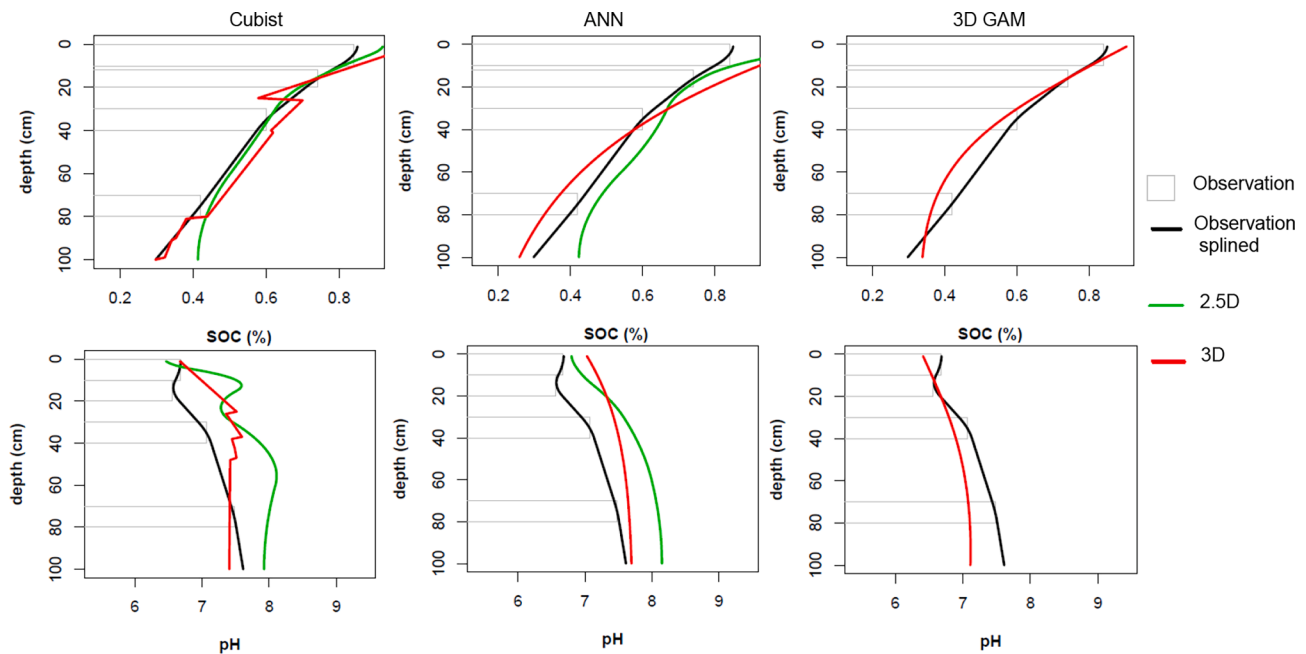


Fig. 4. Plots of 2.5D and 3D predictions versus observed values of SOC (profile: ed108) and pH (profile: na031) using Cubist (left), ANN (middle) and 3D GAM (right) techniques. The grey box is observation, the black line is observation splined, the green line is 2.5D prediction and the red line is the 3D prediction. (For interpretation of the references to colour in this figure legend, the reader is referred to the web version of this article.)

and 5th percentile prediction is referred to as the 90% prediction interval (PI). The 90% PI for SOC prediction of each location was calculated every 1 cm until 1 m and then averaged for a soil profile:

$$\text{Average PI} = \left(\sum_{i=1}^{100} P_{95_i} - P_{5_i} \right) / 100 \quad (3)$$

where P_{95} is the 95% quantile of the prediction (%), P_5 is the 5% quantile of the prediction (%). A high value of average PI for a soil profile indicates that the model produces a high uncertainty.

3. Results

3.1. Edgeroi: Accuracy statistics

Table 2 shows the prediction accuracies including all depths for all machine learning techniques of SOC concentration, pH, clay content and CEC from a validation set of 103 soil profiles in Edgeroi. In general, the validation R^2 and RMSE were similar between 2.5D and 3D models across QRF, Cubist and ANN techniques. All models in 2.5D and 3D have a median R^2 value of 0.39, ranging from 0.29 to 0.54.

SOC and pH have much better validation results compared to clay and CEC across all machine learning techniques. SOC and pH predictions have R^2 values between 0.40 and 0.53 in both 2.5D and 3D models. ANN models in 2.5D and 3D modelling provided best prediction accuracies for clay and CEC with R^2 values around 0.40.

Although there is a slight improvement in accuracy in 2.5D models compared to 3D ones for QRF, Cubist and ANN, the difference is small. Overall, there is no single best model that can produce the most accurate prediction in 2.5D and 3D. Model performances were found to be variable across soil properties.

3.2. Effect of different depth assignment methods for the 3D model

In order to examine the 3D model with different methods to assign point depth values, the vertical distributions of SOC and pH using the QRF model were compared (Fig. 3). Two soil profiles (ed343 for SOC and na036 for pH) were selected as examples.

Both 2.5D and 3D predictions using QRF for SOC and pH revealed positive correlations between predicted and measured values and similar trend with depth. SOC and pH prediction using 3D models seem to have larger variations with depth compared to 2.5D models.

The most striking result is that 3D predictions of SOC and pH showed varying patterns for different point-depth assignment approaches, but all of the predictions displayed a “stepped” trend. The steps were more obvious especially in 3D-B (boundaries depth assignment) and 3D-F (fine discretization) methods. Clay and CEC showed the same “stepped” predictions but with greater error (plots not shown).

3.3. Depth prediction from different prediction models

The trend of prediction with depth was examined further for Cubist, ANN and 3D GAM models for 2.5D and 3D approaches. The 3D-B point-depth assignment method was used in this section. Fig. 4 shows that Cubist model also produced irregular “stepped” predictions with depth for SOC and pH (Fig. 4). A sharp discontinuity prediction with depth was observed in the Cubist model, which is due to the “if-then” rules. Using ensemble Cubist model (adding a number of committees in the model) slightly improved the performance of the Cubist model, though the predictions were still stepped (data not shown).

Both ANN and 3D GAM models provided smooth predictions for SOC, pH, clay and CEC. The ANN model is parametric and thus shows a smooth function, while the GAM model is a smooth interpolator.

For the prediction of clay and CEC, Cubist, ANN and 3D GAM models showed low predictive capacity. The ANN model tended to overpredict low values and underpredict higher values by showing approximate straight-line predictions. The 3D GAM presented decreasing variability and less skewed distributions with depth. Clay and CEC with depth are more variable and are likely to be influenced by geological parent material (Nussbaum et al., 2018; Samuel-Rosa et al., 2015) and soils degree of weathering (chemical weathering) (Smeck et al., 1981), which cannot be well-predicted in this example.

3.4. Prediction of soil carbon stock

The effect of different prediction models on soil carbon stock

Table 3

RMSE from validation of total carbon storage (kg m^{-2}) at different depth intervals (0–30, 0–50 and 0–80 cm) on the pedogenic horizons of the 103 profiles in Edgeroi.

	0–30 cm				0–50 cm				0–80 cm			
	QRF	Cubist	ANN	3D GAM	QRF	Cubist	ANN	3D GAM	QRF	Cubist	ANN	3D GAM
2.5D	1.83	1.82	1.77		2.61	2.58	2.51		3.58	3.53	3.42	
3D-A	1.87	1.91	1.76	1.73	2.69	2.70	2.62	2.50	3.69	3.66	3.71	3.55
3D-B	1.82	1.81	1.76	1.71	2.62	2.61	2.54	2.49	3.57	3.62	3.57	3.55
3D-F	1.79	1.75	1.84	1.73	2.56	2.53	2.66	2.54	3.48	3.49	3.69	3.61

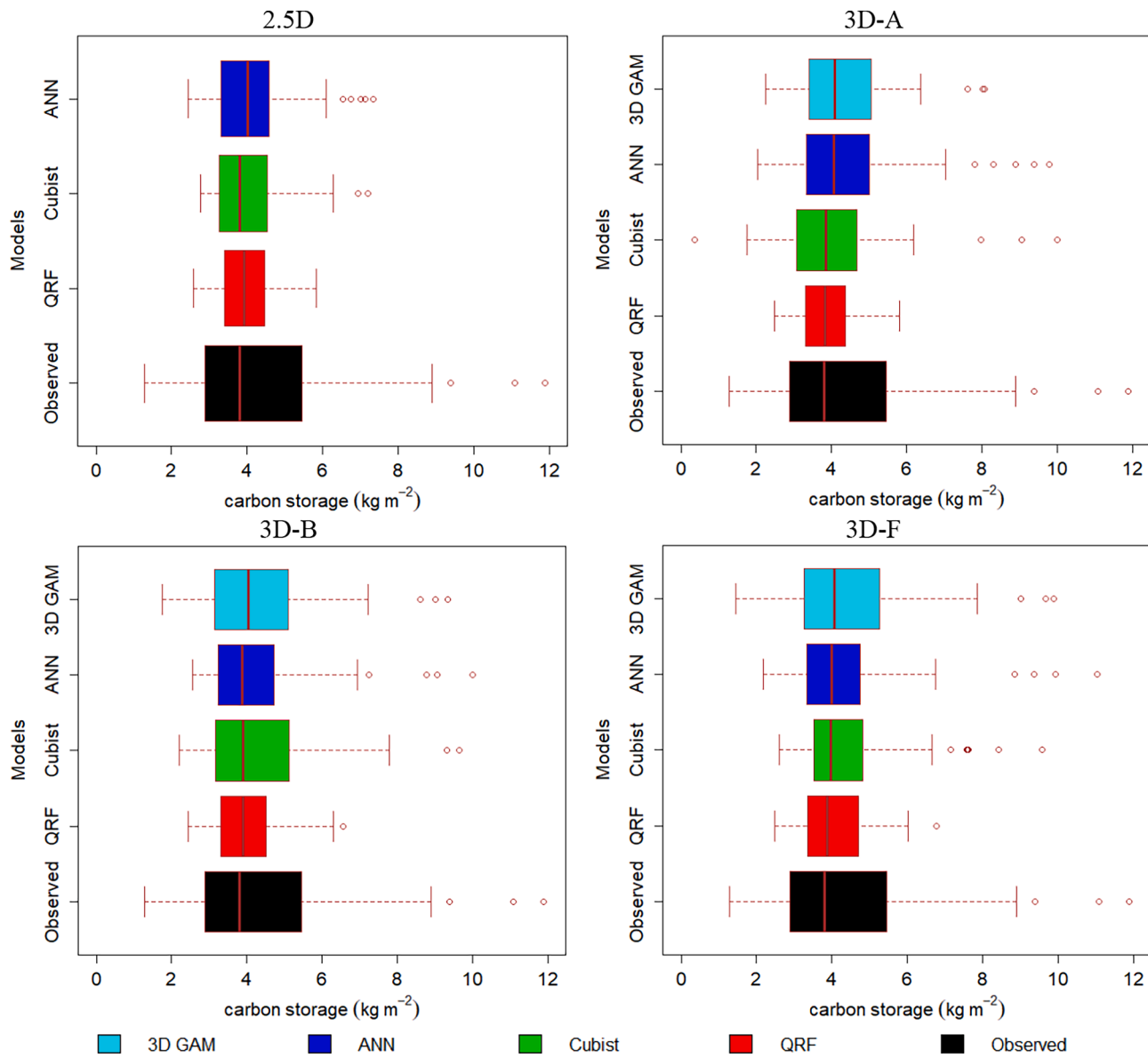


Fig. 5. Boxplots of predictions for carbon storage at 0–30 cm using different models.

estimation at different depth intervals was examined. Table 3 shows the RMSE values for total carbon storage (kg m^{-2}) at 0–30, 0–50 and 0–80 cm using different models. RMSE increased with depth for all 2.5D and 3D models, showing the low predictive capacity with depth. While the 3D GAM models showed the lowest RMSE values for all depth intervals, the accuracy of all models both in 2.5 and 3D are all similar. There is an indication that the 3D GAM model preserves more of the carbon stock distribution (Fig. 5).

3.5. Correlation with depth

Another proposed benefit of the 3D model is that it accounts for the covariation of the soil data within the profile as data for all depths were used as inputs (Viscarra Rossel et al., 2015). To test this proposition, we calculated the correlation matrix of soil properties at the 5 depth intervals. We compared the correlation matrix of the observed and predicted depth interval values. A model that maintains the covariation of soil data with depth will have a similar correlation coefficient with the observed depth data.

Table 4

Correlation matrix of SOC at different depth intervals (0–5, 5–15, 15–30, 30–60 and 60–100 cm) between observations, 2.5D QRF and 3D-A QRF predictions.

	Observation				QRF (2.5D)				QRF (3D-A)			
	0–5	5–15	15–30	30–60	0–5	5–15	15–30	30–60	0–5	5–15	15–30	30–60
5–15	0.92				0.91				0.86			
15–30	0.60	0.85			0.61	0.78			0.73	0.90		
30–60	0.51	0.72	0.91		0.29	0.37	0.76		0.31	0.47	0.78	
60–100	0.29	0.48	0.69	0.86	0.06	0.17	0.56	0.86	0.20	0.34	0.63	0.89

Table 5

Mean absolute difference (MAD) of correlation of soil properties at different depths (0–5, 5–15, 15–30, 30–60 and 60–100 cm) between predictions and observations.

	Model	QRF	Cubist	ANN	3D GAM
SOC	2.5D	0.148	0.259	0.077	
	3D-A	0.114	0.095	0.153	0.110
pH	2.5D	0.085	0.080	0.161	
	3D-A	0.117	0.156	0.142	0.155
Clay	2.5D	0.030	0.029	0.092	
	3D-A	0.079	0.066	0.094	0.090
CEC	2.5D	0.022	0.042	0.052	
	3D-A	0.055	0.061	0.061	0.057

Table 6

Accuracy statistics of 2.5D, QRF in 3D and 3D GAM predictions.

	QRF		3D GAM	
	R ²	RMSE	R ²	RMSE
2.5D	0.36	1.43		
3D-A	0.30	1.50	0.39	1.40

Table 4 displays three correlation matrices of SOC at the depth intervals for the observed and QRF prediction values in Edgeroi. 3D and 2.5D QRF predictions showed similar correlations of SOC between depths. Except for the 60–100 cm, where the 2.5D model showed a low correlation with other depths, overall, 2.5D and 3D models performed similarly.

We further calculated the mean absolute difference (MAD) of correlation coefficients between predicted and observed depth intervals. A model which maintains the covariation of the observed data will have a low MAD value. **Table 5** shows that 3D predictions presented slightly lower MAD of correlation than 2.5D prediction only for SOC when using QRF and Cubist models, but not for other soil properties and other models. For the ANN model, except for soil pH, 2.5D prediction showed lower MAD of correlation compared to 3D prediction.

Overall, although the 3D model maintained a better correlation in a few cases, there is no difference between 2.5D and 3D models. The 2.5D ANN, which is a multi-task model where all depth intervals are predicted simultaneously, seems to preserve a better correlation, especially for SOC.

3.6. Validation in Hunter Valley: QRF and 3D GAM

In order to explore whether the 3D modelling approaches can predict point depth observations, the SOC data from the Hunter Valley were examined using QRF and 3D GAM models and validated against the actual point observations at 2 cm increment.

Since the number of observations is limited (59 soil profiles), profile-based 10-fold cross-validation was used. We converted point observations to depth intervals as inputs and validated against point observations. For the QRF model, 2.5D prediction ($R^2 = 0.36$) was better than 3D ($R^2 = 0.30$). While 3D GAM performed the best in this case with $R^2 = 0.39$ (**Table 6**).

3D QRF model still showed the “stepped” prediction and tended to

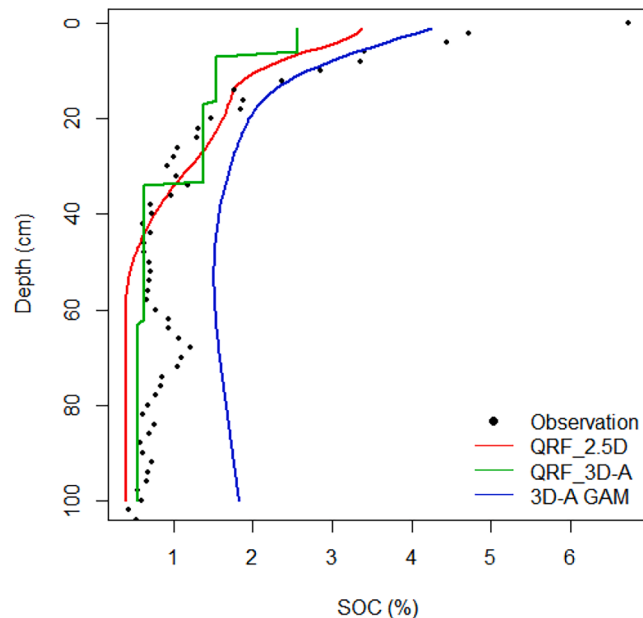


Fig. 6. Plots of 2.5D, 3D QRF and 3D GAM predictions versus observed values of SOC (a Kurosols profile). Black points are observations, the red line is a 2.5D prediction, the green line is 3D QRF prediction and the blue line is 3D GAM prediction. (For interpretation of the references to colour in this figure legend, the reader is referred to the web version of this article.)

overestimate lower values and underestimate higher values across depths. 3D QRF model cannot replicate field point observations values. 3D GAM showed smooth predictions but not able to predict values at deeper depths accurately (**Figs. 4 and 6**).

A problem with predicting soil with depth for all models is that it cannot accurately predict the surface SOC content. **Fig. 6** shows an example where all models underestimate surface SOC content. A future sampling of the surface 0–2 cm seems critical for DSM and monitoring whichever model we use. The surface value represents the largest concentrations of SOC and nutrients with the steepest gradient. Thus, we need to fix the upper boundary condition to improve the prediction.

3.7. Uncertainty analysis in the prediction in Hunter Valley

Fig. 7 presents an example of the 90% PI for the above Kurosols profiles for both 2.5D and 3D models. It shows that the 90% PI value for the 3D model was larger than that of the 2.5D model within a soil profile. The 2.5D model has less prediction uncertainty.

To further assess the model uncertainty, the average PI values for each of the 59 soil profiles were calculated and compared. The density plot in **Fig. 8** shows the distribution of all the average PI values for both 2.5D and 3D models. Average PI values ranged from 1.6 to 5% with a mean value of 2.3% for 2.5D models, whereas the 3D models ranged from 1.8 to 10% with a mean value of 3.2%. In addition to less accurate, the 3D model produces larger uncertainty relative to the 2.5D model.

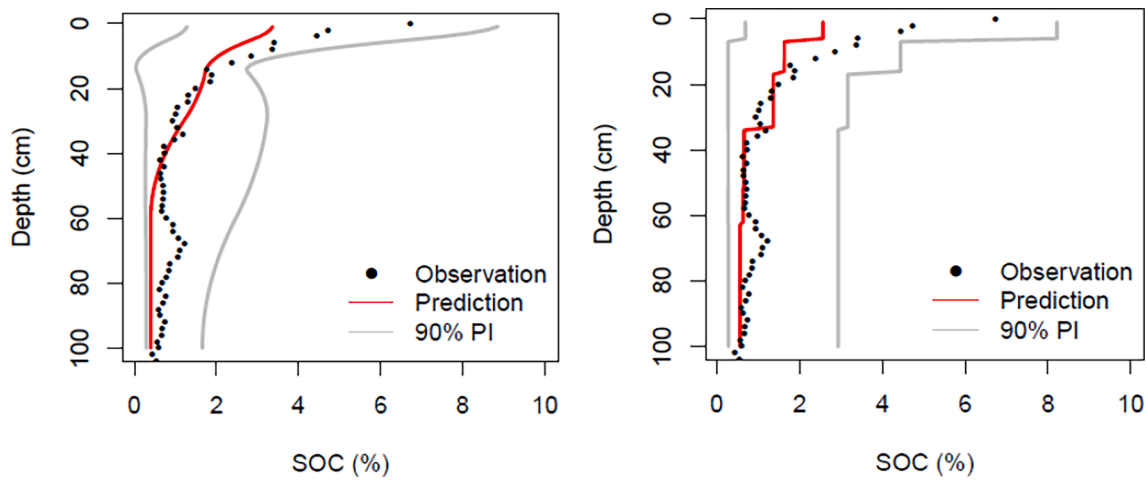


Fig. 7. Plots of 90% PI for SOC of the same Kurosols profile for both 2.5D and 3D models.

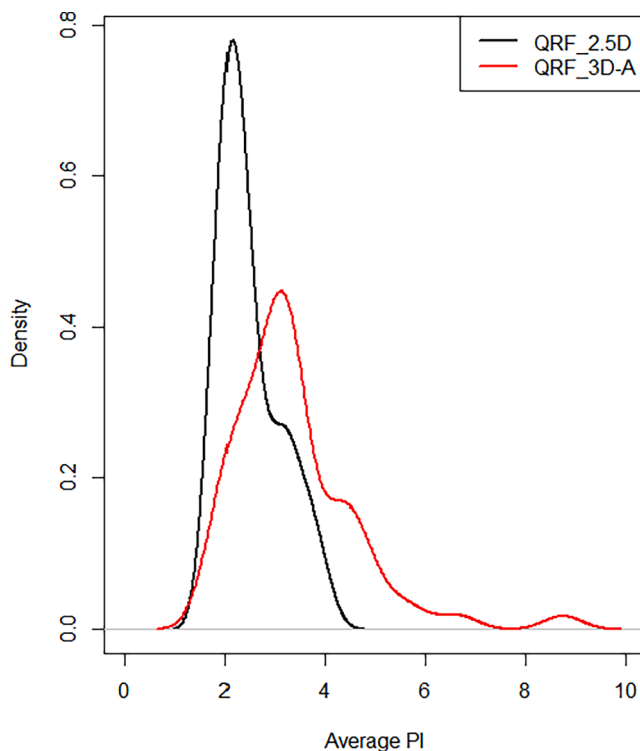


Fig. 8. Kernel density estimate plot for the average PI values between 2.5D and 3D models.

4. Discussion

4.1. Variation in the DSM performances across soil properties

The 2.5D model, which predicts soil properties to pre-determined depth intervals, and 3D model, which predicts a property at a specific point-depth, were compared. The comparison for the Edgeroi area shows that good predictions were obtained for SOC and pH regardless of the models, while predictions of clay and CEC were modest. However, no single best model can produce the most accurate predictions of 2.5D and 3D DSM for all soil properties.

In Edgeroi, prediction using the 2.5D model is not worse than the 3D model, similar to the study of Nauman and Duniway (2019) and Roudier et al. (2020). In terms of R^2 and RMSE, the 2.5D and 3D models using different machine learning techniques produce comparable

performances when validated against depth intervals observations. Even though the 2.5D model has uncertainty due to the assumption of a uniform distribution of soil property within the pre-determined depth interval (Orton et al., 2016), the 3D model including depth as a predictor does not solve this problem. The pragmatic and computational efficiency of 3D models with different point-depth assignment approaches seems appealing, but the validation of R^2 and RMSE for depth interval observations in Edgeroi are similar.

4.2. Artefacts of 3D depth functions

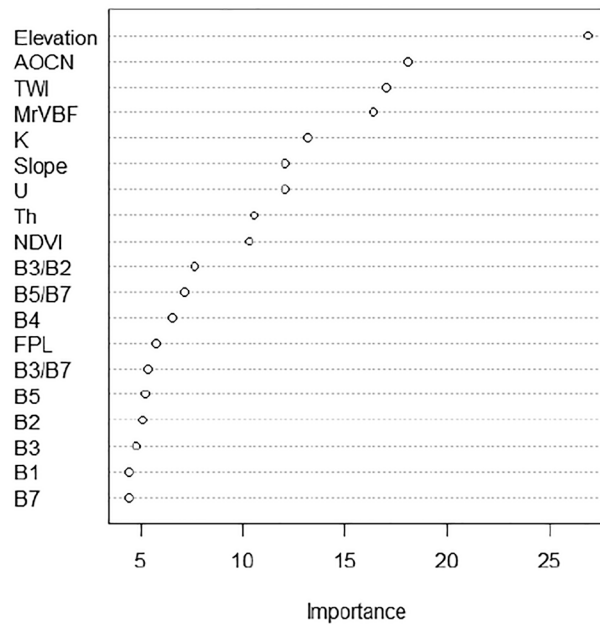
Although the 2.5D and 3D approaches produce a similar accuracy, the 3D tree-based models (i.e., QRF and Cubist) produce “stepped” depth functions. This 3D artefact is important where point (fixed depth) predictions are required (e.g., in biophysical modelling), but less so for integral (depth range) estimates. This is reflected in the prediction of point SOC values in the Hunter Valley, where the 3D model is less accurate and more uncertain. Depth was the most important predictor in all 3D models of both study areas based on the QRF variable importance metrics (Fig. A.1). Due to this, the use of depth as one of the covariates in tree model structures can create higher uncertainty of the prediction. A possible explanation is that the depth variable dominates the tree splits and this condition makes the model less rigorous in formulating the relationship between target soil property and environmental covariates (Nauman and Duniway, 2019).

We acknowledge that non-continuous variations of soil properties across depth may exist, however the stepped depth artefacts are a consequence of the tree algorithms. Recently, Roudier et al. (2020) proposed the use of data augmentation to address this problem. This includes drawing random observations from the depth intervals based on the uncertainty of soil measurements.

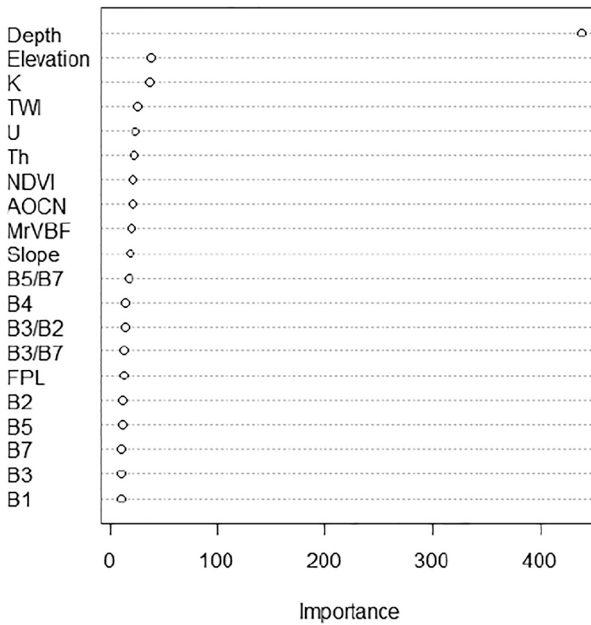
No stepped depth artefacts were found in ANN and 3D GAM models. The ANN model is parametric, while the GAM model is a smooth interpolator. Both of them show smooth predictions and better agreement with the carbon storage data by preserving more mass. Note that the GAM model treats Easting, Northing, and Depth as a coordinate system or trend in the model and not as covariates (Eq. (2)).

An examination of point SOC observations shows that the 3D models cannot replicate point observations. Point 3D soil mapping has lower accuracy, larger uncertainty, and unpredictable behaviour, not producing realistic predictions relative to 2.5D mapping. Thus, 3D soil mapping with depth as a covariate is somewhat contentious. The 3D approach cannot resolve greater detail depth measurement; thus caution should be taken when using 3D modelling approaches to predict a property at a specific point-depth for future DSM studies.

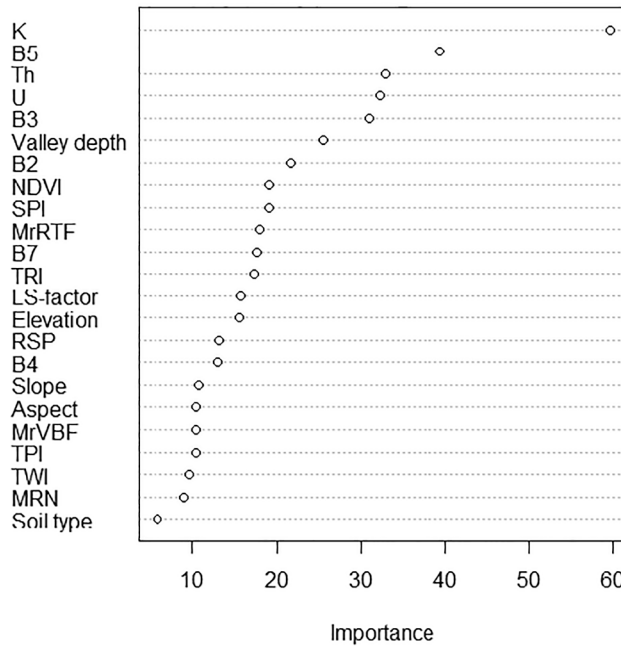
Edgeroi_2.5D



Edgeroi_3D



Hunter Valley_2.5D



Hunter Valley _3D

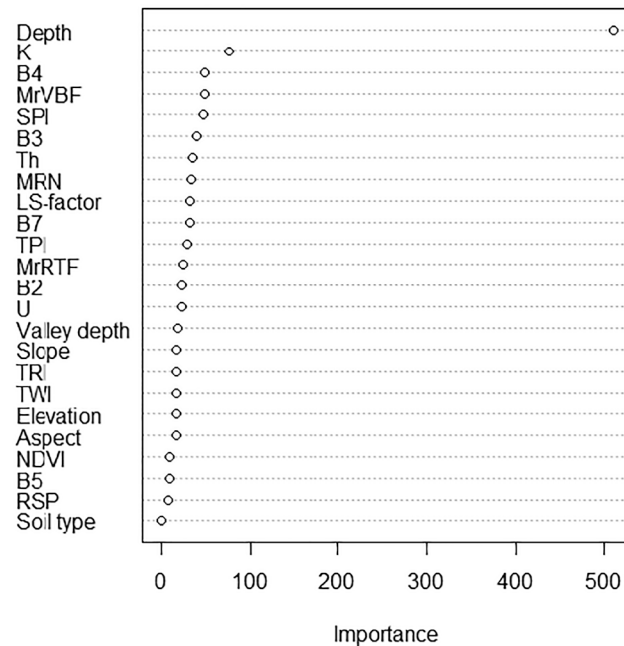


Fig. A1. Importance plots for 2.5D (left) and 3.5D (right) models of SOC in Edgeroi (upper panel) and Hunter Valley (bottom panel) derived using the QRF approach. Covariates were sorted decreasingly from top to bottom by Mean Decrease MSE (mean squared error). The higher Mean Decrease MSE value for the variable the more important it is in the model.

4.3. Model selection and future works

With respect to the usage requirement, there is no single best method that can be recommended for 3D mapping of soil properties. 3D models are efficient and could be used to predict values at various depth interval requirements (e.g., 0–10 or 0–20 or 0–30 or 0–40 cm). The impact of the unbalanced contributions of covariates in the 3D approach (depth was much more important than any other covariates) deserves a future mathematical study.

3D GAM can address the 3D component of soil processes by treating depth as a trend, not a covariate. Since 3D GAM is a smooth interpolator,

it does not present stepped artefacts generated by tree models. Multi-tasking ANN is able to model soil properties at various depth intervals simultaneously (Padarian et al., 2019) which was demonstrated in this study better for soil carbon stock estimates due to the better preservation of mass.

Soil observations usually have limited depth measurements, generally between 2 and 5 measurements per profile. And thus, we cannot expect models to produce finer depth resolution data. Effort should be focused on more efficiently collecting depth data via sensors, such as in the field using portable X-ray fluorescence (pXRF) (Weindorf et al., 2014) capable of quantifying and identifying chemical elemental

concentrations in soils or in the laboratory more efficient spectrometer measurements (Ng et al., 2020). Such soil information has been successfully used to predict soil properties (Andrade et al., 2020; Sharififar et al., 2019; Silva et al., 2016; Tang et al., 2020). O'Rourke et al. (2016) found that XRF spectra is more effective to predict total carbon, soil organic carbon and pH when compared to the direct use of elemental concentrations. In addition, the exploration of sampling of the surface layers (e.g., 0–2 cm) seems critical for further DSM and model monitoring schemes.

5. Conclusions

This paper examines the vertical distribution for soil properties using 2.5D and 3D models using different point-depth assignment approaches. We concluded that:

- (1) 2.5D and 3D models' accuracy is similar.
- (2) 3D soil mapping can present an unpredictable behaviour with depth, often not producing realistic predictions relative to 2.5D mapping.
- (3) 3D soil mapping using tree-based models can produce "stepped" depth functions.
- (4) 3D modelling cannot replicate point soil variation with depth.
- (5) 3D soil mapping with depth as a covariate requires caution with respect to the prediction method and use requirement. Developing a pedology-driven model would be more beneficial than a data-driven approach.
- (6) A future sampling of the surface 0–2 cm seems critical for DSM and monitoring for whichever model we use.

Declaration of Competing Interest

The authors declare that they have no known competing financial interests or personal relationships that could have appeared to influence the work reported in this paper.

Acknowledgements

The authors acknowledge Philippe Lagacherie (INRA Montpellier) for his helpful comments that improved the discussion section. Budiman Minasny and Laura Poggio are members of the Research Consortium GLADSOILMAP supported by LE STUDIUM Loire Valley Institute for Advanced Studies.

References

- Adhikari, K., Hartemink, A.E., Minasny, B., Kheir, R.B., Greve, M.B., Greve, M.H., 2014. Digital mapping of soil organic carbon contents and stocks in Denmark. *PLoS ONE* 9, e105519.
- Akpa, S.I.C., Odeh, I.O.A., Bishop, T.F.A., Hartemink, A.E., 2014. Digital mapping of soil particle-size fractions for Nigeria. *Soil Sci. Soc. Am. J.* 78, 1953–1966.
- Andrade, R., Silva, S.H.G., Faria, W.M., Poggere, G.C., Barbosa, J.Z., Guilherme, L.R.G., Curi, N., 2020. Proximal sensing applied to soil texture prediction and mapping in Brazil. *Geoderma Regional* 23, e00321.
- Arrouays, D., Grundy, M.G., Hartemink, A.E., Hempel, J.W., Heuvelink, G.B.M., Hong, S.Y., 2014. In: GlobalSoilMap: toward a fine-resolution global grid of soil properties. *Advances in agronomy* Academic Press, pp. 93–134.
- Behrens, T., Förster, H., Scholten, T., Steinrücken, U., Spies, E.-D., Goldschmitt, M., 2005. Digital soil mapping using artificial neural networks. *J. Plant Nutr. Soil Sci.* 168, 21–33.
- Bishop, T.F.A., McBratney, A.B., Laslett, G.M., 1999. Modelling soil attribute depth functions with equal-area quadratic smoothing splines. *Geoderma* 91 (1–2), 27–45.
- Breiman, L., 2001. Random forests. *Machine Learning* 45 (1), 5–32.
- Fajardo, M., McBratney, A.B., Whelan, B., 2016. Fuzzy clustering of Vis–NIR spectra for the objective recognition of soil morphological horizons in soil profiles. *Geoderma* 263, 244–253.
- Filippi, P., Jones, E.J., Bishop, T.F.A., 2020. Catchment-scale 3D mapping of depth to soil sodicity constraints through combining public and on-farm soil databases – A potential tool for on-farm management. *Geoderma* 374, 114396.
- Filippi, P., Jones, E.J., Ginnis, B.J., Whelan, B.M., Roth, G.W., Bishop, T.F.A., 2019. Mapping the depth-to-soil pH constraint, and the relationship with cotton and grain yield at the within-field scale. *Agronomy* 9 (5), 251.
- Geosciences Australia, 2008. Radiometric data of the Narrabri, Moree, Inverell and Manilla 1:250 000 topographic map sheets. In: (Geophysical Archive Data Delivery System (GADDS)). <http://www.geoscience.gov.au/bin/mapserv36?map=/public/http://www.geoportal/gadds/gadds>.
- Grimm, R., Behrens, T., Märker, M., Elsenbeer, H., 2008. Soil organic carbon concentrations and stocks on Barro Colorado Island — Digital soil mapping using Random Forests analysis. *Geoderma* 146, 102–113.
- Hastie, T., Tibshirani, R., 1986. Generalized additive models. *Statistical Science* 1, 297–318.
- Hastie, T.J., Tibshirani, R.J., 1990. Generalized additive models. Chapman and Hall, London.
- Hawley, S., Glen, R., Baker, C., 1995. Newcastle Coalfield Regional Geology 1: 100 000. Geological Survey of New South Wales, Sydney, Australia.
- Hengl, T., de Jesus, J.M., Heuvelink, G.B.M., Gonzalez, M.R., Kilibarda, M., Blagotić, A., Shangguan, W., Wright, M.N., Geng, X., Bauer-Marschallinger, B., 2017. SoilGrids250m: Global gridded soil information based on machine learning. *PLoS ONE* 12 (2), e0169748.
- Hengl, T., de Jesus, J.M., MacMillan, R.A., Batjes, N.H., Heuvelink, G.B.M., Ribeiro, E., Samuel-Rosa, A., Kempen, B., Leenaars, J.G.B., Walsh, M.G., Gonzalez, M.R., 2014. SoilGrids1km — global soil information based on automated mapping. *PLoS ONE* 9, e105992.
- Hengl, T., MacMillan, R.A., 2019. Predictive Soil Mapping with R. OpenGeoHub foundation, Wageningen, the Netherlands, 370 pages, www.soilmapper.org.
- Hole, F.D., 1953. Suggested terminology for describing soils as three-dimensional bodies. *Soil Science Society of America, Proceedings* 17, 131–135.
- Isbell, R.F., 2002. *The Australian Soil Classification*. CSIRO Publishing, Melbourne.
- IUSS Working Group WRB, 2014. World Reference Base for Soil Resources 2014. International Soil Classification System for Naming Soils and Creating Legends for Soil Maps, World Soil Resources Reports No. 106, FAO, Rome.
- Kempen, B., Brus, D.J., Stoorvogel, J.J., 2011. Three-dimensional mapping of soil organic matter content using soil type-specific depth functions. *Geoderma* 162, 107–123.
- Kidd, D., Webb, M., Malone, B.P., Minasny, B., McBratney, A.B., 2015. Eighty-metre resolution 3D soil attribute maps for Tasmania, Australia. *Soil Res.* 53, 932–955.
- Kuhn, M., Weston, S., Keefer, C., Coulter, N., 2018. Package Cubist: Rule- and Instance-Based Regression Modeling. (R package version 0.2.2).
- Kuhn, M.K., Weston, S., Keefer, C., Coulter, N., 2016. Cubist Models for Regression.
- Lacoste, M., Minasny, B., McBratney, A.B., Michot, D., Viaud, V., Walter, C., 2014. High resolution 3D mapping of soil organic carbon in a heterogeneous agricultural landscape. *Geoderma* 213, 296–311.
- Liau, A., Wiener, M., 2018. Package: randomForest. Title: Breiman and Cutler's Random Forests for Classification and Regression. (R package version: 4.6–14).
- Liu, F., Rossiter, D.G., Song, X.D., Zhang, G.L., Yang, R.M., Zhao, Y.G., Li, D.C., Ju, B., 2016. A similarity-based method for three dimensional prediction of soil organic matter concentration. *Geoderma* 263, 254–263.
- Ma, Y.X., Minasny, B., Malone, B.P., McBratney, A.B., 2019a. Pedology and digital soil mapping (DSM). *Eur. J. Soil Sci.* 70, 216–235.
- Ma, Y.X., Minasny, B., Welivitiya, W.D.D.P., Malone, B.P., Willgoose, G.R., McBratney, A.B., 2019b. The feasibility of predicting the spatial pattern of soil particle-size distribution using a pedogenesis model. *Geoderma* 341, 195–205.
- Malone, B.P., 2018. Package itirh. Soil data and some useful associated functions. (R Package Version 1.0.).
- Malone, B.P., McBratney, A.B., Minasny, B., Laslett, G.M., 2009. Mapping continuous depth functions of soil carbon storage and available water capacity. *Geoderma* 154, 138–152.
- Malone, B.P., Odgers, N.P., Stockmann, U., Minasny, B., McBratney, A.B., 2018. Digital mapping of soil classes and continuous soil properties. In: McBratney, A.B., Minasny, B., Stockmann, U. (Eds.), *Pedometrics*. Springer, Sydney.
- McBratney, A.B., Field, D.J., Koch, A., 2014. The dimensions of soil security. *Geoderma* 213, 203–213.
- McBratney, A.B., Mendonca Santos, M.L., Minasny, B., 2003. On digital soil mapping. *Geoderma* 117, 3–52.
- McGarry, D., Ward, W.T., McBratney, A.B., 1989. Soil Studies in the Lower Namoi Valley: Methods and Data. The Edgeroi Dataset. CSIRO Division of Soils, Adelaide, 2 vols.
- Meinshausen, N., 2006. Quantile Regression Forests. *Journal of Machine Learning Research* 7, 983–999.
- Meinshausen, N., 2017. Package quantregForest. Quantile Regression Forests. (R package version 1.3–7).
- Minasny, B., McBratney, A.B., 2002. The neuro-m method for fitting neural network parametric pedotransfer functions. *Soil Sci. Soc. Am. J.* 66, 352–361.
- Minasny, B., McBratney, A.B., 2006. A conditioned Latin hypercube method for sampling in the presence of ancillary information. *Comput. Geosci.* 32, 1378–1388.
- Minasny, B., McBratney, A.B., 2016. Digital soil mapping: A brief history and some lessons. *Geoderma* 264, 301–311.
- Minasny, B., McBratney, A.B., Mendonca-Santos, M.L., Odeh, I.O.A., Guyon, B., 2006. Prediction and digital mapping of soil carbon storage in the Lower Namoi Valley. *Aust. J. Soil Res.* 44, 233–244.
- Mishra, U., Lal, R., Slater, B., Calhoun, F., Liu, D.-S., Meirvenne, M.V., 2009. Predicting soil organic carbon stock using profile depth distribution functions and ordinary kriging. *Soil Sci. Soc. Am. J.* 73 (2), 614–621.
- Nauman, T.W., Duniway, M.C., 2019. Relative prediction intervals reveal larger uncertainty in 3D approaches to predictive digital soil mapping of soil properties with legacy data. *Geoderma* 347, 170–184.
- Ng, W., Husnain, Anggria, L., Siregar, A.F., Hartatik, W., Sulaiman, Y., Jones, E., Minasny, B., 2020. Developing a soil spectral library using a low-cost NIR spectrometer for precision fertilization in Indonesia. *Geoderma Regional* 22, e00319.

- Nussbaum, M., Spiess, K., Baltensweiler, A., Grob, U., Keller, A., Greiner, L., Schaeppman, M.E., Papritz, A., 2018. Evaluation of digital soil mapping approaches with large sets of environmental covariates. *SOIL* 4, 1–22.
- O'Rourke, S.M., Stockmann, U., Holden, N.M., McBratney, A.B., Minasny, B., 2016. An assessment of model averaging to improve predictive power of portable vis-NIR and XRF for the determination of agronomic soil properties. *Geoderma* 279, 31–44.
- Orton, T.G., Pringle, M.J., Bishop, T.F.A., 2016. A one-step approach for modelling and mapping soil properties based on profile data sampled over varying depth intervals. *Geoderma* 262, 174–186.
- Orton, T.G., Pringle, M.J., Bishop, T.F.A., Menzies, N.W., Dang, Y.P., 2020. Incremental kriging for 3-D modelling and mapping soil properties: Combining machine learning and geostatistical methods. *Geoderma* 361, 114094.
- Padarian, J., Minasny, B., McBratney, A.B., 2019. Using deep learning for digital soil mapping. *SOIL* 5, 79–89.
- Padarian, J., Minasny, B., McBratney, A.B., 2020. Machine learning and soil sciences: a review aided by machine learning tools. *SOIL* 6 (1), 35–52.
- Poggio, L., Gimona, A., 2014. National scale 3D modelling of soil organic carbon stocks with uncertainty propagation — An example from Scotland. *Geoderma* 232–234, 284–299.
- Quinlan, J.R., 1992. Learning with continuous classes., Proc. In: of the Fifth Australian Joint Conference on Artificial Intelligence World Scientific, pp. 343–348.
- R Development Core Team, 2017. R: A Language and Environment for Statistical Computing. R Foundation for Statistical Computing, Vienna, Austria.
- Ramcharan, A., Hengl, T., Nauman, T., Brungard, C., Waltman, S., Wills, S., Thompson, J., 2018. Soil property and class maps of the conterminous United States at 100-meter spatial resolution. *Soil Sci. Soc. Am. J.* 82 (1), 186–201.
- Roudier, P., Burge, O.R., Richardson, S.J., McCarthy, J.K., Grealish, G.J., Ausseil, A.G., 2020. National Scale 3D Mapping of Soil pH Using a Data Augmentation Approach. *Remote Sensing. Remote Sensing* 12, 2872.
- Samuel-Rosa, A., Heuvelink, G.B.M., Vasques, G.M., Anjos, L.H.C., 2015. Do more detailed environmental covariates deliver more accurate soil maps? *Geoderma* 243–244, 214–227.
- Saunders, A.M., Boettinger, J.L., 2006. Incorporating classification trees into a pedogenic understanding raster classification methodology, Green River Basin, Wyoming, USA. In: Lagacherie, P., McBratney, A.B., Voltz, M. (Eds.), *Digital SoilMapping: An Introductory Perspective*. Elsevier, Amsterdam, The Netherlands, pp. 389–399.
- Sharififar, A., Singh, K., Jones, E., Gingit, F.I., Minasny, B., 2019. Evaluating a low-cost portable NIR spectrometer for the prediction of soil organic and total carbon using different calibration models. *Soil Use Manag.* 35 (4), 607–616.
- Silva, S.H.G., Poggere, G.C., Menezes, M.D.d., Carvalho, G.S., Guilherme, L.R.G., Curi, N., 2016. Proximal Sensing and Digital Terrain Models Applied to Digital Soil Mapping and Modeling of Brazilian Latosols (Oxisols). *Remote Sensing* 8(8), 614.
- Smeck, N.E., Ritchie, A., Wilding, L.P., Drees, L.R., 1981. Clay accumulation in soils of poorly drained soils of western Ohio. *Soil Sci. Soc. Am. J.* 45, 95–102.
- Tang, Y., Jones, E., Minasny, B., 2020. Evaluating low-cost portable near infrared sensors for rapid analysis of soils from South Eastern Australia. *Geoderma Regional* 20, e00240.
- Triantafyllis, J., McBratney, A.B., 1993. Application of continuous methods of soil classification and land suitability assessment in the lower Namoi valley. CSIRO, Australia.
- Veronesi, F., 2012. 3D Advance mapping of soil properties. Doctoral dissertation Thesis, Cranfield University, Cranfield, UK.
- Viscarra Rossel, R.A.V., Chen, C., Grundy, M.J., Searle, R., Clifford, D., Campbell, P.H., 2015. The Australian three-dimensional soil grid: Australia's contribution to the GlobalSoilMap project. *Aust. J. Soil Res.* 53 (8), 845–864.
- Wadoux, A.M.J.-C., Padarian, J., Minasny, B., 2019. Multi-source data integration for soil mapping using deep learning. *SOIL* 5, 107–119.
- Ward, W.T., 1999. Soils and landscapes near Narrabri and Edgeroi, New South Wales, with data analysis using fuzzy k-means.
- Weindorf, D.C., Bakr, N., Zhu, Y.-D., 2014. Advances in portable X-ray fluorescence (PXRF) for environmental, pedagogical, and agronomic applications. . In: H. Yang, B. Kuang, A.M. Mouzan (Eds.), *Advances in Agronomy*, pp. 1–45.
- Wood, S., 2019. Package mgcv. Mixed GAM Computation Vehicle with Automatic Smoothness Estimation. (R package version: 1.8–28).
- Zhang, Y., Ji, W., Saurette, D.D., Easher, T.H., Li, H., Shi, Z., Adamchuk, V.I., Biswas, A., 2020. Three-dimensional digital soil mapping of multiple soil properties at a field-scale using regression kriging. *Geoderma* 366, 114253.